B and T Cells Are Not Required for the *viable motheaten* Phenotype

By Calvin C. K. Yu,*§ Hing-Wo Tsui,*‖ Bo Y. Ngan,‡ Marc J. Shulman,* Gillian E. Wu,*§ and Florence W. L. Tsui*‖

*From the Departments of *Immunology and ‡Pathology, University of Toronto, Toronto M5S 1A8; the §Wellesley Hospital Research Institute, Toronto M4Y 1J3; and the ‖Toronto Hospital Research Institutes, Toronto, Ontario, Canada M5T 2S8*

Summary

Hematopoietic cell phosphatase (HCP), encoded by the *hcph* gene, (also called PTP1C, SHP, SH-PTP1, and PTPN6) is deficient in *motheaten (me/me)*, and the allelic *viable motheaten* (me^v/me^v) mice. Since HCP is expressed in many cell types and protein phosphorylation is a major mechanism of regulating protein function, it is not surprising that the *motheaten* phenotype is pleiotropic. It is commonly thought that immune system involvement causes this disease. If so, the *motheaten* disease ought to be alleviated when the recombination activation gene-1 (*RAG-1*) is disrupted because there will be no V(D)J rearrangement and thus impaired development of B and T cells. We bred homozygous, double-mutant me^v/me^v·*RAG-1*$^{-/-}$ mice and found that, in fact, they developed full-blown *motheaten* inflammatory disease, including pneumonitis, alopecia, inflamed paws, and splenomegaly with elevated myelopoiesis. Thus, except for autoantibodies, the *motheaten* phenotype does not depend on the presence of B and T cells. This observation cautions the use of *motheaten* mice as a model of autoimmune disease.

Protein tyrosine kinases and phosphatases play a major role in protein tyrosine phosphorylation, a process that regulates cell growth and proliferation. Some understanding of the physiological role of particular protein kinases and phosphatases can be inferred from the phenotype of mutant animals. In the case of hematopoietic cell phosphatase (HCP)[1] (1–5), which is deficient in mice homozygous for the *motheaten* (*me/me*) mutations (6–8), the mutant phenotypes have been intensively studied. The *me/me* mice and the allelic me^v/me^v mice are severely immunodeficient. In both *motheaten* mutants, maturations of B and T lymphocytes are impaired. Both *me/me* and *viable motheaten* (me^v/me^v) mice also develop the so-called autoimmune diseases characterized by patchy alopecia (hence the name) (9, 10), inflamed paws (11), and hypergammaglobulinemia (12). Typically, their serum has high titers of autoreactive antibodies (9–13), and immune complexes are present in various tissues, such as the skin, lung, and kidney (10). The mutant animals died prematurely, usually of pneumonitis characterized by the accumulation of macrophages, lymphocytes, and granulocytes in the lungs (10, 14).

Since systemic autoimmune diseases usually result from complex interactions among lymphoid (B and T) cells and target tissues, it is difficult to distinguish the contribution of each cell type in the initiation of the autoimmune response and the induction of specific pathological lesions. The presence of lymphocytes and complexes in affected tissues in both *motheaten* mutants has suggested that the immune system might contribute importantly to the *motheaten* phenotype. This hypothesis predicts that the *motheaten* phenotype will be alleviated by disruption in the recombination activation gene-1 (*RAG-1*), a null mutation that prevents V(D)J rearrangement and thus prevents development of antigen specific B and T cells (15). To test this prediction, we generated and studied double-mutant mice, me^v/me^v *RAG-1*$^{-/-}$. The me^v/me^v *RAG-1*$^{-/-}$ mutant mice develop disease characteristic of the *motheaten* phenotype, including pneumonitis, inflammation of the skin and extremities, and splenomegaly with elevated myelopoiesis. Thus, except for autoantibodies, all manifestations of the *motheaten* disease occur in the absence of B and T cells.

Materials and Methods

Mice. The founding C57BL/6J $+/me^v$ mice were obtained from The Jackson Laboratory (Bar Harbor, ME), and the founding *RAG-1*$^{-/-}$ mice were kindly provided by S. Tonegawa (Massachusetts Institute of Technology, Cambridge, MA). Mice were maintained at the animal facility of the Ontario Cancer Institute (Toronto), and kept in microisolator housing units (Lab Products, Maywood, NJ) in rooms equipped with the Hepa-filtered air handling system. Cages, bedding, and water were sterilized by autoclaving, and food was sterilized by γ-irradiation. Mice were handled by aseptic forceps or aseptic gloves.

[1] *Abbreviations used in this paper:* HCP, hematopoietic cell phosphatase; *me/me, motheaten* mice; me^v/me^v, *viable motheaten* mice; *RAG-1*, recombination activation gene-1; SSCP, single-strand conformation polymorphism.

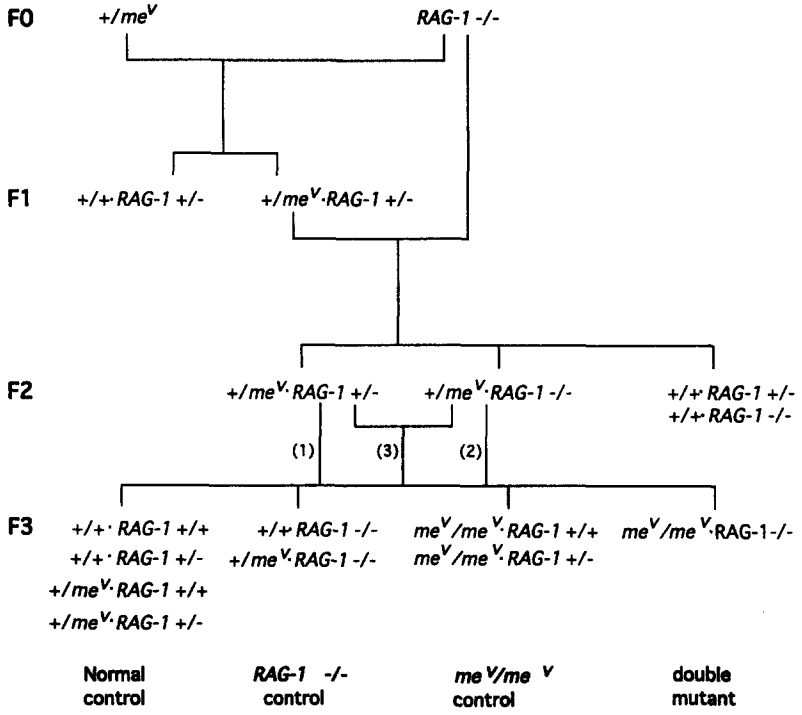

Figure 1. Generation of mice with various genotypes at the *me*^{v} and *RAG-1* loci. Since *me*^{v}/*me*^{v} mice are sterile, mice heterozygous at the *me*^{v} locus were used for breeding. The founding +/*me*^{v} and *RAG-1*$^{-/-}$ parents were from the C57BL/6J and 129/Sv × CD1 backgrounds, respectively. The F1 +/*me*^{v}·*RAG-1*$^{+/-}$ mice were back-crossed to the *RAG-1*$^{-/-}$ parent to generate the F2 generation. The F2 mice were then intercrossed to generate the F3 generation, which were obtained by the following crosses: (*1*) cross among the +/*me*^{v}·*RAG-1*$^{+/-}$ mice, (*2*) cross among the +/*me*^{v}·*RAG-1*$^{-/-}$ mice, and (*3*) cross between the +/*me*^{v}·*RAG-1*$^{+/-}$ mice and +/*me*^{v}·*RAG-1*$^{-/-}$ mice. The F3 generation consisted of mice of all possible genotypes, i.e., the normal control mice (i.e., mice that have at least one wild-type allele at each of the *me*^{v} and *RAG-1* loci), the *RAG-1*$^{-/-}$ control mice (i.e., mice that are homozygous for the *RAG-1* null mutation and have at least one wild-type allele at the *me*^{v} locus), the *me*^{v}/*me*^{v} control mice (i.e., mice that are homozygous for the *me*^{v} mutation and have at least one wild-type allele at the *RAG-1* locus), and the double-mutant mice (i.e., mice that are homozygous for both the *me*^{v} mutation and *RAG-1* null mutation).

Genetic Testing. The strategy used for typing the *me*^{v} locus was to amplify the region of the genome containing the *me*^{v} mutation by PCR and then to examine the amplified products by single-strand conformation polymorphism (SSCP) analysis. The primers used for amplifying a 167-bp fragment in which the *me*^{v} mutation is located were 5′-TGTCATCGTCATGACTACC-3′ and 5′-TCAGGCTTGGCAGCAAACTCG-3′. The latter primer was kinased with [^{33}P]ATP. PCR conditions used were 15 s at 94°C, 15 s at 54°C, and 15 s at 72°C for 30 cycles. The amplified products were then subject to SSCP analysis: a portion of the PCR product was boiled for 3 min, quickly chilled on ice, loaded on an MDE (J.T. Baker Chemical Co., Phillipsburg, NJ) gel, and run at 3 W for 19 h. The gel was dried, and the DNA was visualized by autoradiography.

The *RAG-1* locus was typed by PCR of the region of the genome containing the disruption in *RAG-1*. The primers used for amplifying an 809-bp *RAG-1* fragment present only in the wild-type allele were 5′-ATCTCCTGCCAGATATGCGAA-3′ and 5′-AACCTCTTCGAATGGTATCT-3′. The primers used for amplifying a 477-bp *neo* fragment present only in the *RAG-1* disrupted allele were 5′-ATGATTGAACAAGATGGATTGC-3′ and 5′-TCCAGATCATCCTGATCGAC-3′. The PCR conditions used were 15 s at 94°C, 15 s at 61°C, and 30 s at 72°C. The extension time was increased by 3 s per cycle for a total of 30 cycles. The amplified DNA was subjected to agarose gel electrophoresis and then visualized by fluorescence of ethidium bromide under ultraviolet light.

Flow Cytometry. Cells taken from 5-wk-old mice were stained with FITC-conjugated anti–IgM heavy chain (33.60) (16), FITC-conjugated anti-CD4 (RM4-5; PharMingen, San Diego, CA), PE-conjugated anti-CD8α (53-6.7; PharMingen), and PE-conjugated anti–Mac-1 (MI/70; Biosource International, Camarillo, CA) antibodies separately. Briefly, 2 × 10^{5} cells were incubated with the appropriate antibodies (1 μg/10^{6} cells) in 100 μl PBS plus 5% FCS (GIBCO BRL, Gaithersburg, MD) for 20 min on ice. The

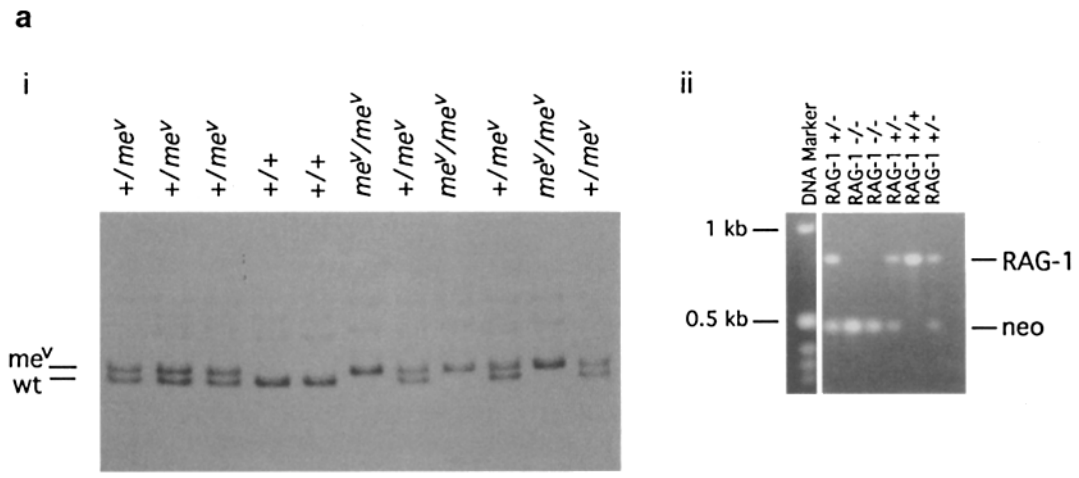

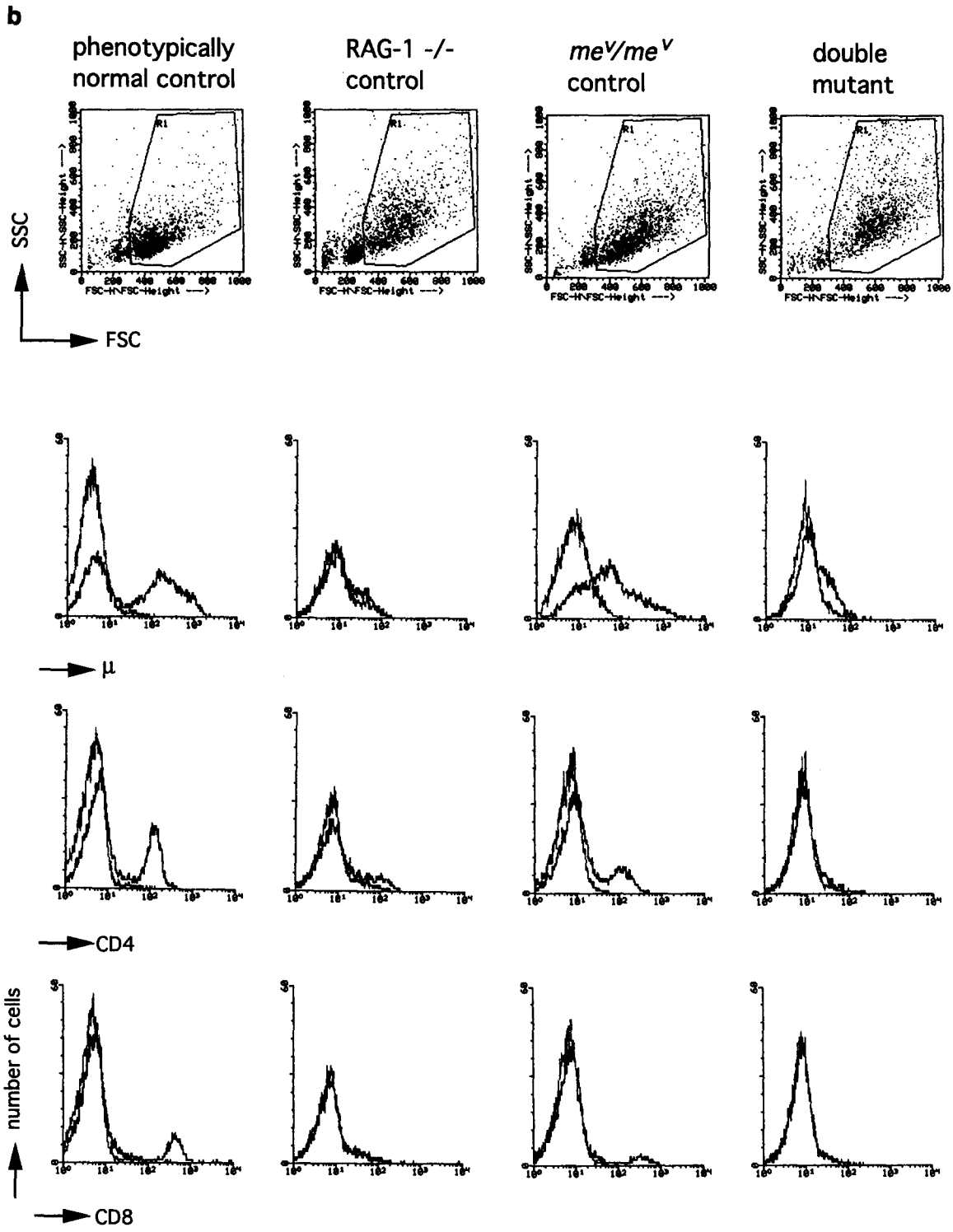

Figure 2. (*a*) Genetic typing identified mutant mice with different genotypes by the distinct DNA patterns. (*b*) Flow cytometry analysis indicates that the B and T cell–specific surface markers μ, and CD4, CD8α, respectively, are not detectable on the spleen cells obtained from the double-mutant and *RAG-1*$^{-/-}$ control. Analysis was carried out on live cells, i.e., the cells included by the R1 gate on the forward scatter (*FSC*) vs. side scatter (*SSC*) profile. 3–6-wk-old mice were analyzed.

stained cells were then washed with PBS plus 5% FCS, and were analyzed by flow cytometry.

Histological Analysis. Tissues were taken from mice of various ages (from 1 to 15 wk). Cross-sections of 4–8-μm thick were obtained from wax-embedded tissue samples and stained with hematoxylin and eosin. Representative sections of the different tissues are shown in Figs. 5 and 6.

Statistical Analysis. The statistical significance of differences

Table 1. *Characteristics of the motheaten and RAG-1 Mutants**

	Motheaten $^{+/\bullet}$ *RAG-1* $^{+/\bullet}$	*Motheaten* $^{+/\bullet}$ *RAG-1* $^{-/-}$	*Motheaten* $^{v/v}$ *RAG-1* $^{+/\bullet}$	*Motheaten* $^{v/v}$ *RAG-1* $^{-/-}$
Median life span‡ (d)	>275 (n = 49)	190 (n = 80)	72 (n = 16)	97 (n = 31)
Skin: focal alopecia§	0/48	0/79	8/13	9/23
Extremities: swelling and lesions‖	0/48	0/79	11/13	19/29
Lung abnormalities¶:	4/9	8/12	5/7	12/12
Inflammation**	4/9	8/12	3/7	11/12
Intraalveolar erythrocytes	1/9	2/12	3/7	5/12
Mϕ with crystalline material‡‡	0/9	0/12	0/7	8/12
Spleen: splenomegaly§§	1/8	1/10	7/7	7/10

*+/• denotes at least one wild-type allele; v denotes the allele carrying the *viable motheaten* mutation.
‡Survival analyses indicate that the double-mutant and the me^v/me^v control do not differ significantly in the probability of survival at any given time (see Fig. 3).
§Difference between the me^v/me^v control and double-mutant is not significant (P = 0.299 in Fisher's exact test).
‖Difference between the me^v/me^v control and double-mutant is significant (P = 0.047 in Fisher's exact test).
¶Lungs scored abnormally if they contained one or more of the three pathological characteristics, i.e., inflammation, intraalveolar erythrocytes, and Mϕ with crystalline material.
**Difference between the me^v/me^v control and double-mutant is significant (P = 0.038 in Fisher's exact test).
‡‡Difference between the me^v/me^v control and double-mutant is significant (P = 0.006 in Fisher's exact test).
§§Splenomegaly was scored by visual inspection.

between sample means was based on Cox regression analysis (for survival analysis), chi square (χ^2) test (for genotype analysis), and Fisher's exact test (for all other analyses). In all tests, differences are treated as significant when $P < 0.05$.

Results

Generation and Analysis of Mutant Mice. The breeding scheme and designation of the various control mice are described in Fig. 1. We analyzed 30 informative litters. The genotype of each mouse was determined by DNA PCR and SSCP analysis for the me^v locus and by PCR for the *RAG-1* locus (Fig. 2 *a*). When mice were killed, the genotypes were verified by flow cytometry, analyzing spleen cells with antibodies recognizing the IgM heavy chain (μ), CD4, CD8α, and Mac-1 (Figs. 2 *b* and 6 *e*). Litter sizes ranged from 1 to 12, and the frequencies of the various genotypes were not significantly different from the expected Mendelian frequencies, i.e., 0.150 of the mice were me^v/me^v control (expected frequency = 0.149, n = 107, χ^2 P >0.900), and 0.194 of the mice were double mutant (expected frequency = 0.155, n = 160, χ^2 P >0.250). The expected frequencies are calculated by taking into account of the various types of crossing that were carried out to generate a given genotype. For example, double-mutant mice were obtained from three types of crossing (see Fig. 1), i.e., (1) $+/me^v \cdot RAG\text{-}1^{+/+} \times +/me^v \cdot RAG\text{-}1^{+/-}$, with a P = 0.0625 for generating the double mutant; (2) $+/me^v \cdot RAG\text{-}1^{-/-} \times +/me^v \cdot RAG\text{-}1^{-/-}$, with a P = 0.25 for generating the double mutant; and (3) $+/me^v \cdot RAG\text{-}1^{+/-} \times +/me^v \cdot RAG\text{-}1^{-/-}$, with P = 0.125 for generating the double mutant. A total of 35 mice were generated from the type 1 crossing, 56 mice from the type 2 crossing, and 69 mice from the type 3 crossing. The expected frequency of generating the double mutant is therefore [(35)(0.0625)+(56)(0.25)+(69)(0.125)]/160=0.155. There was no significant difference between the observed and expected frequencies of the various mutant mice carrying the me^v/me^v genotype. Thus, there seems to be little selection against the me^v/me^v mice in utero whether or not *RAG-1* is expressed.

Effect on Life Span. Each mouse was also examined for characteristics normally present in mice defective in HCP: shortened life span, dermatitis, inflammatory lesions in the extremities, hemorrhagic pneumonitis, and extramedullary myelopoiesis sites. The median life span of the double mutants (97 d) was similar to that of the me^v/me^v control (72 d) but substantially shorter than that of the $RAG\text{-}1^{-/-}$ control (190 d) and normal control (>275 d) (Table 1). By using the proportional hazard model and Cox regression analysis (Fig. 3 and reference 17), which take into account the mice that were alive, killed, and dead at the end of the study, we are able to conclude that the absence of *RAG-1* expression does not significantly affect the probability of survival of the me^v/me^v mice at any given time.

Dermatitis in $me^v/me^v \cdot RAG\text{-}1^{-/-}$ Mice. Severe dermatitis with patchy alopecia is the hallmark of the *motheaten* phenotype (9, 10). Both the me^v/me^v control and double-mutant mice in our study manifested the disease with ruffled, "spotty" fur, indicating irregular hair growth (Fig. 4 *a–d*). 9 out of 23 double-mutant mice and 8 out of 13 me^v/me^v control mice had these skin lesions (Table 1). Since the frequency of skin lesions in the double mutant is not significantly different from that in the me^v/me^v control, the skin lesions in the me^v/me^v mice are not caused by B or T cells.

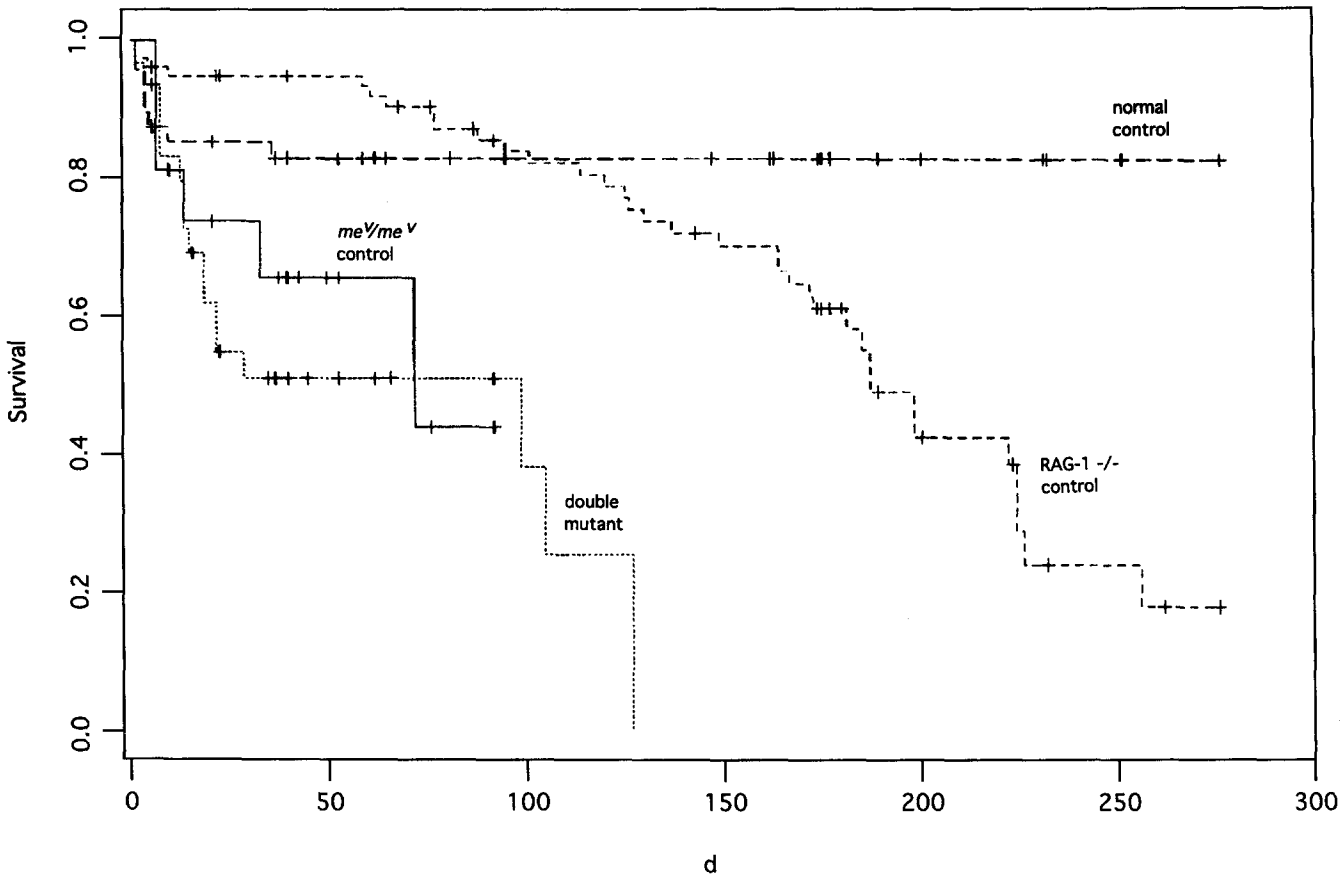

Figure 3. Survival curve of mice with the various genotypes. The proportional hazard model using the Cox regression analysis indicates that, at any given time, the probability of survival of the double-mutant is not significantly different from that of the me^v/me^v control ($P > 0.540$). However, the probability of survival of the double mutant is significantly lower than that of the $RAG\text{-}1^{-/-}$ control ($P < 0.001$) and the normal control ($P < 0.001$). There is weak evidence of a difference in the probability of survival between the $RAG\text{-}1^{-/-}$ control and the normal control ($P > 0.070$).

Inflammatory Lesions in the Extremities. Both the me^v/me^v control and double-mutant mice developed the characteristic inflammation in the paws: extensive swelling and open pustular lesions. The paw lesions typically appeared between 5 and 10 d after birth, and the severity of these swellings and lesions was of the same magnitude (Fig. 4, *e–g*). The frequencies of paw deformities in the me^v/me^v control (11 of 13) and double-mutant mice (19 of 29) were similar (Table 1). The reason for incomplete penetrance of these symptoms is unknown, but may be caused by a variation in the time of onset of the disease.

Lung Abnormalities. Lung abnormalities characteristic of pneumonitis were present in ~70% of the me^v/me^v control and in all double-mutant mice examined (Table 1). These pneumonitis-like characteristics were the likely cause of death of these mice during the first few months of life (Table 1 and Fig. 3). Histological analysis revealed severe inflammation in the lungs of both me^v/me^v control and double-mutant mice (Table 1 and Fig. 5 *c–e*). A proportion of the normal control and $RAG\text{-}1^{-/-}$ control mice had some inflammation (Table 1), but it was a much milder form than that in the lungs of the me^v/me^v control and double-mutant mice (Fig. 5, *a* and *b*). A large amount of crystalline material, which appears to be associated with degradation of erythrocytes (10), is present inside the alveolar macrophages of the double-mutant mice. This abnormality has also been observed by Shultz (10), who reported crystalline material in macrophages in the C57BL/6J me^v/me^v mice. The reason for their absence in the me^v/me^v control in the present study is unknown. Since the me^v/me^v control mice in our study are of a mixed genetic background (see Fig. 1), however, strain-specific factors may modulate the severity of the lung abnormalities. No crystalline material was detected in the lung sections of the $RAG\text{-}1^{-/-}$ control or normal control (Table 1). These results lead to the conclusion that in the absence of B and T cells, me^v/me^v mice develop severe hemorrhagic pneumonitis.

Extramedullary Myelopoiesis. Elevated myelopoiesis in the spleen of the C57BL/6 me^v/me^v mice results in splenomegaly (10). In the present study, the incidence of splenomegaly was similar in the me^v/me^v control and double-mutant mice (Table 1). The spleens of these mice generally had no organized white pulp (Fig. 6 *a–d*) and contained more than fivefold higher numbers of myeloid cells, as detected by anti–Mac-1 antibody, than the normal control and $RAG\text{-}1^{-/-}$ control mice (Fig. 6 *e*).

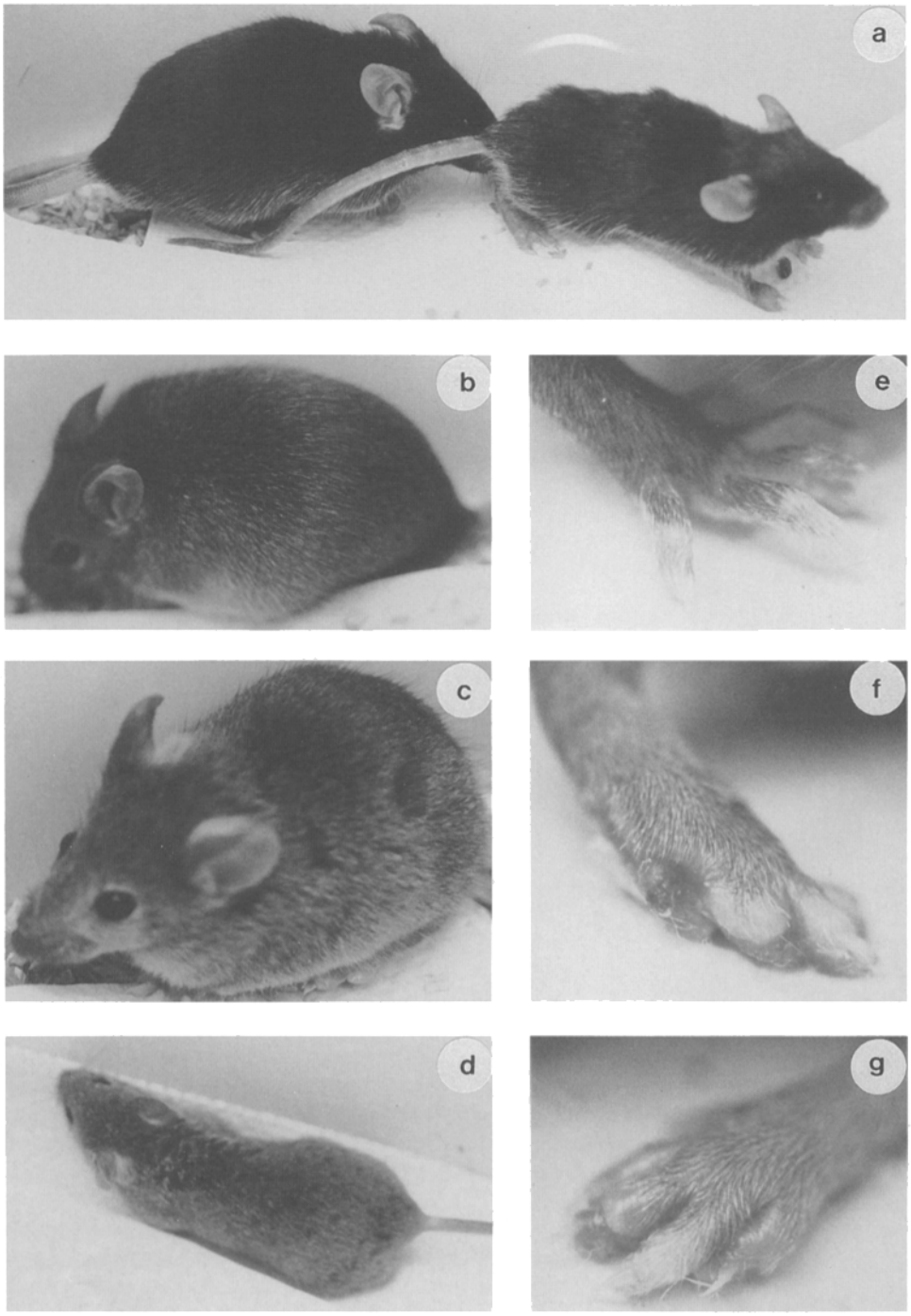

Figure 4. Double-mutant and me^v/me^v control mice have similar gross phenotypes. Inflammation in the skin is evident from the "spotty" fur: (*a*) C57BL/6J $+/me^v$ mouse (*left*) has smooth, shiny fur, whereas the congenic C57BL/6J me^v/me^v mouse (*right*) has ruffled fur interspersed with patchy alopecia; (*b*) $RAG\text{-}1^{-/-}$ control has normal-looking fur; (*c*) me^v/me^v control and (*d*) double-mutant mice have ruffled fur with "spots," indicating irregular hair growth. Normal paws are found in (*e*) $RAG\text{-}1^{-/-}$ control mice, whereas swollen paws with lesions were found in (*f*) me^v/me^v control and (*g*) double-mutant mice.

Discussion

Since the *RAG-1* mutation used in the present study completely and specifically blocks the development of B and T cells, our results indicate that except for the production of autoantibodies, the manifestations of the *motheaten* inflammatory disease occur in the absence of the antigen-specific arm of the immune system. Contrary to our findings, Shultz and Sidman (18) reported that the me^v/me^v *scid*/*scid* mice had a threefold increase in life span as compared to the me^v/me^v mice. This difference in life span might be because the effects of the *scid* mutation are not limited to B and T cells (19, 20). Moreover, earlier studies using mouse mutations that partially block either B or T lymphopoiesis are consistent with our analysis of the completely B- and T-deficient $me^v/me^v \cdot RAG\text{-}1^{-/-}$ mutant mice. Scribner et al. (21) and Shultz (14) observed that neither the presence of the *xid* mutation, which impairs the production of

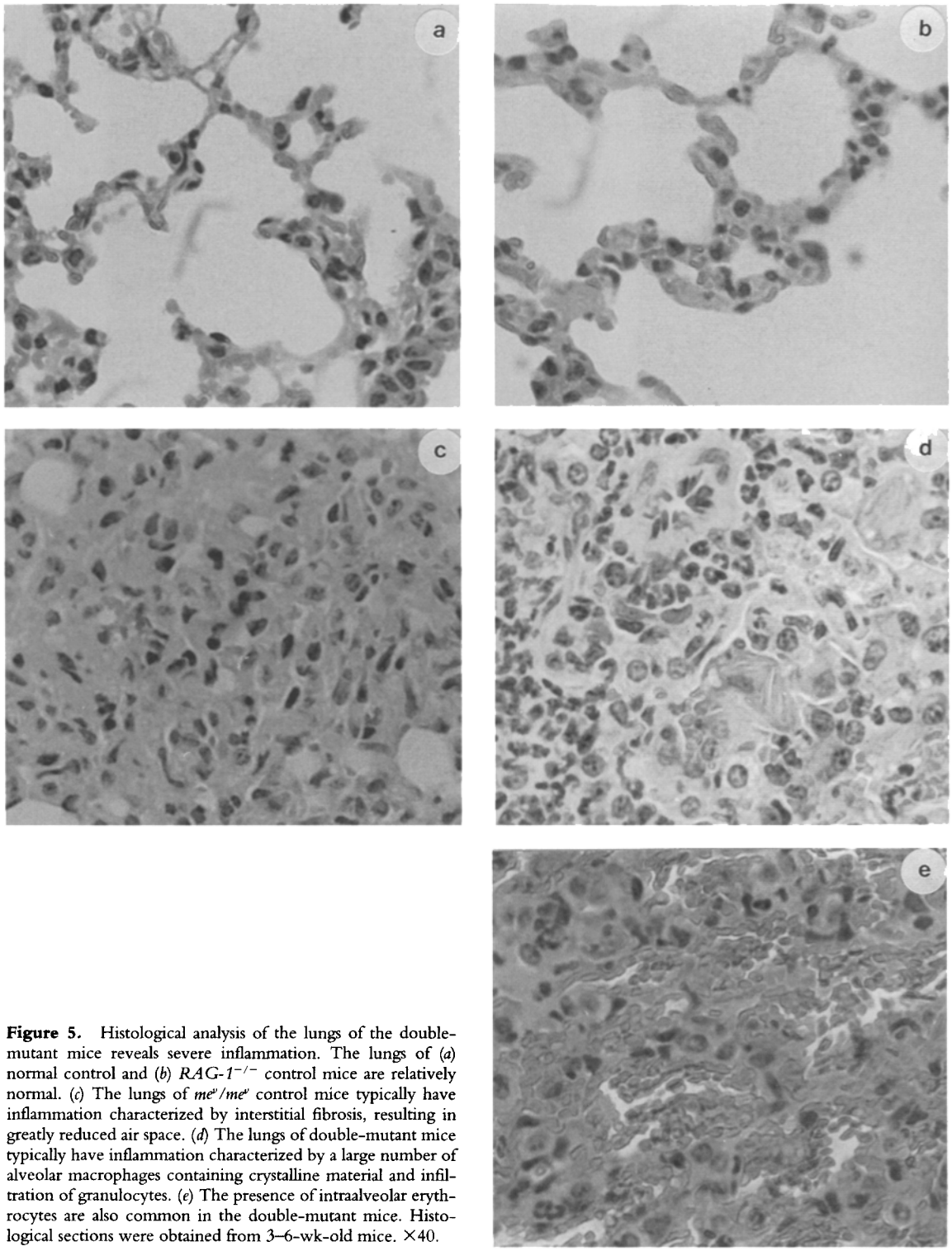

Figure 5. Histological analysis of the lungs of the double-mutant mice reveals severe inflammation. The lungs of (*a*) normal control and (*b*) *RAG-1*$^{-/-}$ control mice are relatively normal. (*c*) The lungs of *me*^{v}/*me*^{v} control mice typically have inflammation characterized by interstitial fibrosis, resulting in greatly reduced air space. (*d*) The lungs of double-mutant mice typically have inflammation characterized by a large number of alveolar macrophages containing crystalline material and infiltration of granulocytes. (*e*) The presence of intraalveolar erythrocytes are also common in the double-mutant mice. Histological sections were obtained from 3–6-wk-old mice. ×40.

CD5^{+} B cells, nor the presence of the *nude* mutation, which blocks T cell development, prevented the manifestations of the *motheaten* phenotype, respectively. These studies, although informative, did not generate a definitive conclusion about the role of B and T cells in the *motheaten* disease, since neither the *xid* nor the *nude* mutation ablates both functional B and T cells (22–25). However, our analysis taken together with these previous studies argues that the *motheaten* phenotype does not require B and T cells. Altogether, these observations call into question the use of *me*/*me* and *me*^{v}/*me*^{v} mice as a paradigm of autoimmune disease.

The exact cell lineages responsible for the *motheaten* dis-

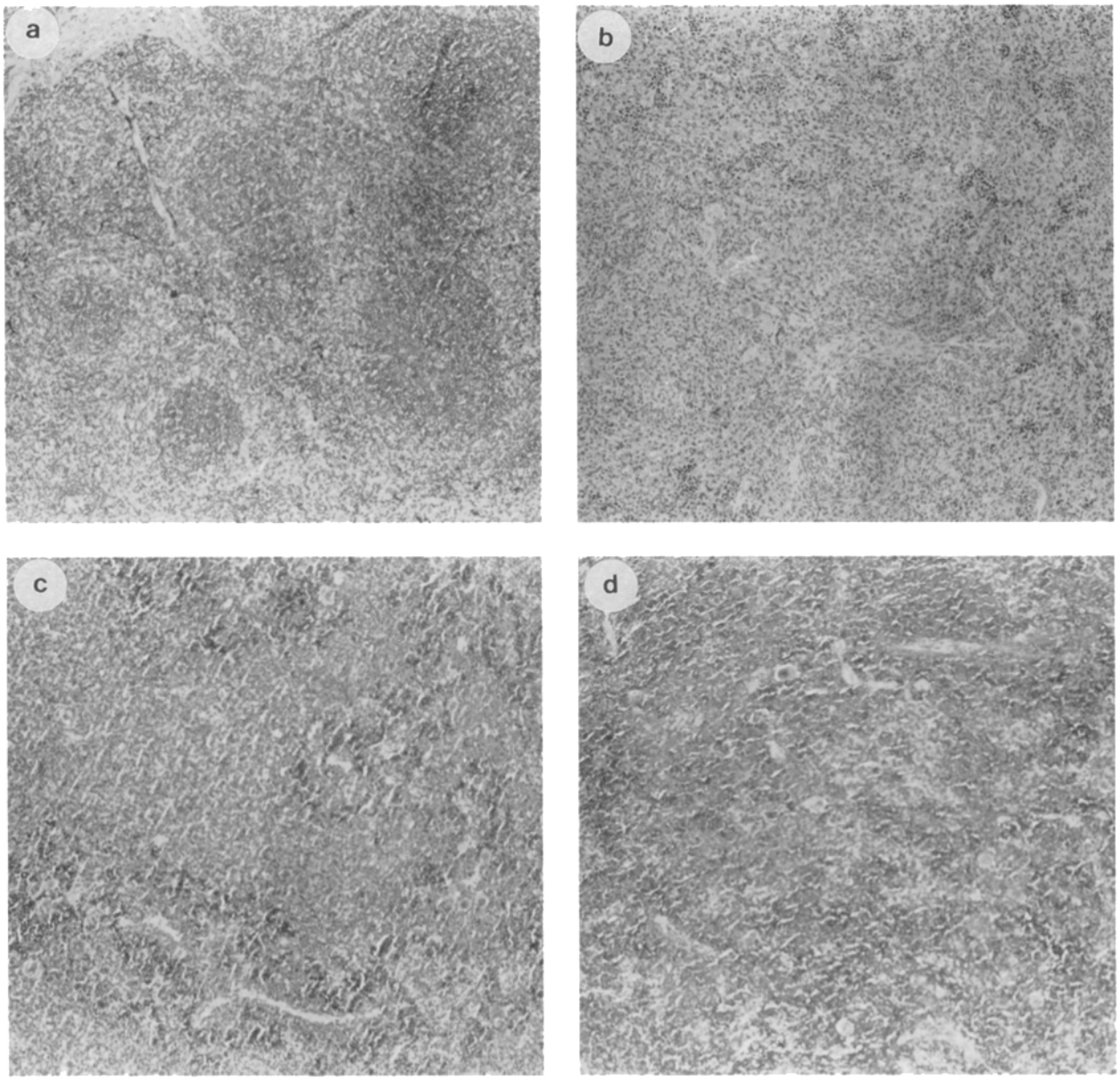

Figure 6. Extramedullary myelopoiesis of the me^v/me^v control and the double-mutant mice. (*a*) The white pulps in the spleen of the normal control are well structured. No organized white pulp is observed in the (*b*) $RAG\text{-}1^{-/-}$ control, (*c*) me^v/me^v control, or (*d*) double-mutant mice. (*e*) Large absolute numbers of cells stained positive for Mac-1 are present in the me^v/me^v control and double-mutant mice. In comparison, the spleens of the normal control and $RAG\text{-}1^{-/-}$ control have low absolute numbers of the Mac-1^+ cells, although the frequency of these cells is high in the $RAG\text{-}1^{-/-}$ control because of the absence of B and T cells. Analysis was carried out on live cells (see Fig. 2 *b*). The error bars of the histograms are SE values from two experiments. Spleens were obtained from 3–6-wk-old mice for analysis.

ease are not known. Infiltration of the affected mouse organs by monocytes, macrophages, and granulocytes suggest that these cell types are the primary effectors of inflammation in the me^v/me^v mice. Consistent with this notion is the observation that treatment with an antibody against CD11b, a subunit of Mac-1 whose expression is restricted to mononuclear phagocytes, granulocytes, and NK cells (26, 27) inhibits inflammation in me^v bone marrow chimeric mice (11). Since the NK cells of me^v mice have virtually no activity and are present at only 30–50% of the normal levels (28), the CD11b study suggests that myeloid cells are responsible for the inflammatory disease of the *me/me* mice (11).

Cells of nonhematopoietic origin may also contribute to the *motheaten* diseases. Although HCP is expressed predominantly in bone marrow, thymus, and hematopoietic cell lines (3, 4, 29), it is detected in low abundance in a few epithelial cell lines and nonhematopoietic cancer cell lines (4, 29). Mutating HCP in a cell-specific manner should delineate the cell types that are important in the manifestation of the *motheaten* disease.

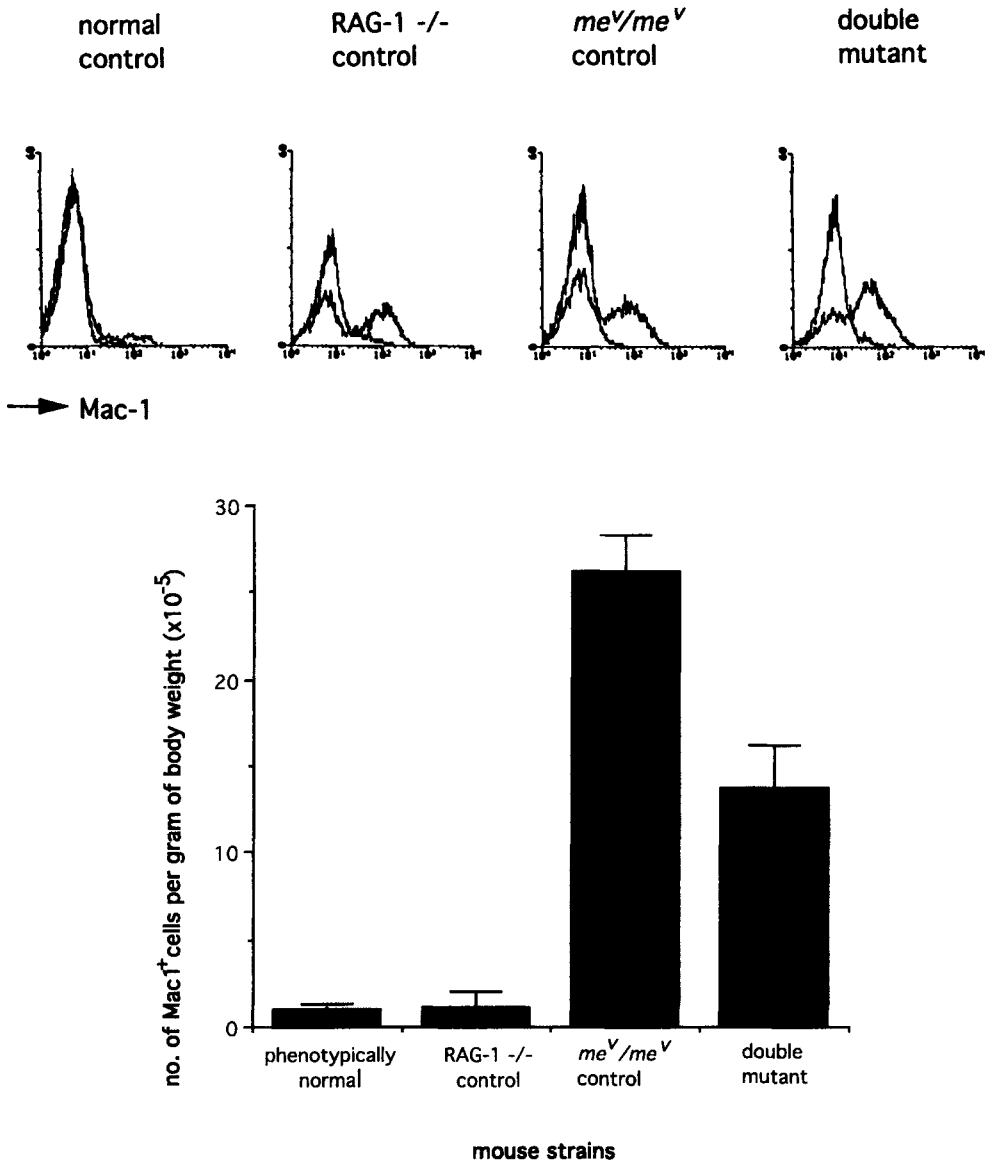

We thank Ruth Croxford and Dr. Charley Steinberg for statistical analyses of data, and Dr. Christopher Paige for helpful discussions.

This work was supported by grants from the Medical Research Council of Canada, the National Cancer Institute of Canada, and the Terry Fox Marathon of Hope. G. Wu is a Medical Research Council Scientist.

Address correspondence to Gillian Wu, Wellesley Hospital Research Institute, Seventh Floor Bruce Wing, 160 Wellesley St. E., Toronto, Ontario, Canada M4Y 1J3.

Received for publication 12 July 1995 and in revised form 7 September 1995.

References

1. Yi, T., D.J. Gilbert, N.J. Jenkins, N.G. Copeland, and J.N. Ihle. 1992a. Assignment of a novel protein tyrosine phosphatase gene (*hcph*) to mouse chromosome 6. *Genomics*. 14: 793–795.

2. Shen, S.-H., L. Bastein, B.I. Posner, and P. Chretien. 1991. A protein-tyrosine phosphatase with sequence similarity to the SH2 domain of the protein-tyrosine kinases. *Nature (Lond.)*. 352:736–739.

3. Matthews, R.J., D.B. Bowne, E. Flores, and M.L. Thomas. 1992. Characterization of hematopoietic intracellular protein tyrosine phosphatases: description of a phosphatase containing an SH2 domain and another enriched in proline-, glutamic acid-, serine-, and threonine-rich sequences. *Mol. Cell. Biol.* 12:2396–2405.
4. Plutzky, J., B.G. Neel, and R.D. Rosenberg. 1992a. Isolation of a src homology 2-containing tyrosine phosphatase. *Proc. Natl. Acad. Sci. USA.* 89:1123–1127.
5. Plutzky, J., B.G. Nell, R.D. Rosenberg, R.L. Eddy, M.G. Byers, J. Jani-Sait, and T.B. Shows. 1992b. Chromosomal localization of an SH2-containing tyrosine phosphatease (PTPN6). *Genomics.* 13:869–870.
6. Tsui, H.W., K.A. Siminovitch, L. de Souza, and F.W.L. Tsui. 1993. *Motheaten* and *viable motheaten* mice have mutations in the haematopoietic cell phosphatase gene. *Nature Genetics.* 4:124–129.
7. Shultz, L.D., P.A. Schweitzer, T.V. Rajan, T. Yi, J.N. Ihle, R.J. Matthews, M.L. Thomas, and D.R. Beier. 1993. Mutations at the murine motheaten locus are within the hematopoietic cell protein-tyrosine phosphatase (*Hcph*) gene. *Cell.* 73:1445–1454.
8. Kozlowski, M., I. Mlinaric-Rascan, G.-S. Feng, R. Shen, T. Pawson, and K.A. Siminovitch. 1993. Expression and catalytic activity of the tyrosine phosphatase PTP1C is severely impaired in motheaten and viable motheaten mice. *J. Exp. Med.* 178:2157–2163.
9. Green, M.C., and L.D. Shultz. 1975. *Motheaten*, an immunodeficient mutant of the mouse. I. Genetics and pathology. *J. Hered.* 66:250–258.
10. Shultz, L.D., D.R. Coman, C.L. Bailey, W.G. Beamer, and C.L. Sidman. 1984. "Viable motheaten," a new allele at the motheaten locus. I. Pathology. *Am. J. Pathol.* 116:179–192.
11. Koo, G.C., H. Rosen, A. Sirotina, X.-D. Ma, and L.D. Shultz. 1993. Anti-CD11b antibody prevents immunopathologic changes in viable moth-eaten bone marrow chimeric mice. *J. Immunol.* 151:6733–6741.
12. Shultz, L.D., and M.C. Green. 1976. *Motheaten*, an immunodeficient mutant of the mouse. II. Depressed immune competence and elevated serum immunoglobulins. *J. Immunol.* 116:936–943.
13. Sidman, C.L., L.D. Shultz, R.R. Hardy, K. Hayakawa, and L.A. Herzenberg. 1986. Production of immunoglobulin isotypes by Ly-1$^+$ B cells in viable motheaten and normal mice. *Science (Wash. DC).* 232:1423–1425.
14. Shultz, L.D. 1988. Pleiotropic effects of deleterious alleles at the "motheaten" locus. *Curr. Top. Microbiol. Immunol.* 137: 216–222.
15. Mombaerts, P., J. Iacomini, R.S. Johnson, K. Herrup, S. Tonegawa, and V.E. Papioannou. 1992. RAG-1-deficient mice have no mature B and T lymphocytes. *Cell.* 68:869–877.
16. Grutzmann, R. 1981. Vergleichende idiotypische Analyse von Rezeptoren mit Spezifitat fur Histokompatibilitatsantigene. Ph.D. Thesis. University of Cologne, Cologne, Germany.
17. Cox, D.R. 1984. Analysis of Survival Data. Chapman & Hall, London. 201 pp.
18. Shultz, L.D., and C.L. Sidman. 1987. Genetically determined murine models of immunodeficiency. *Annu. Rev. Immunol.* 5: 367–403.
19. Fulop, G.M., and R.A. Phillips. 1990. The scid mutation in mice causes a general defect in DNA repair. *Nature (Lond.).* 347:479–482.
20. Hendrickson, E.A., X. Qin, E.A. Bump, D.G. Shatz, M. Oettinger, and D.T. Weaver. 1991. A link between double-stranded break-related repair and V(D)J recombination: the *scid* mutation. *Proc. Natl. Acad. Sci. USA.* 88:4061–4065.
21. Scribner, C.L., C.T. Hansen, D.M. Klinman, and A.D. Steinberg. 1987. The interaction of the *xid* and *me* genes. *J. Immunol.* 138:3611–3617.
22. DeSousa, M.A.B., D.M. Parrott, and E.M. Pantelouris. 1969. The lymphoid tissues in mice with congenital aplasia of the thymus. *Clin. Exp. Immunol.* 4:637–644.
23. Kindred, B. 1979. Nude mice in immunology. *Prog. Allergy.* 26:137–238.
24. Scher, I. 1982. The CBA/N mouse strain: an experimental model illustrating the influence of the X-chromosome on immunity. *Adv. Immunol.* 33:1–71.
25. Wicker, L.S., and I. Scher. 1986. X-linked immune deficiency (*xid*) of CBA/N mice. *Curr. Top. Microbiol. Immunol.* 124:87–101.
26. Springer, T., G. Galfre, G.S. Secher, and C. Milstein. 1979. Mac-1: a macrophage differentiation antigen identified by monoclonal antibody. *Eur. J. Immunol.* 9:301.
27. Ault, K.A., and T.A. Springer. 1981. Cross-reaction of a rat anti-mouse phagocyte-specific monoclonal antibody (anti-Mac-1) with human monocytes and natural killer cells. *J. Immunol.* 126:359–364.
28. Koo, G.C., C.L. Manyak, J. Dasch, L. Ellingsworth, and L.D. Shultz. 1991. Suppressive effects of monocytic cells and transforming growth factor-β on natural killer cell differentiation in autoimmune *viable motheaten* mutant mice. *J. Immunol.* 147:1194–1200.
29. Yi, T., J.L. Cleveland, and J.N. Ihle. 1992b. Protein tyrosine phosphatase containing SH2 domains: characterization, preferential expression in hematopoietic cells, and localization to human chromosome 12p12-p13. *Mol. Cell. Biol.* 12:836–846.